Supplement of Atmos. Chem. Phys., 22, 10409–10423, 2022
https://doi.org/10.5194/acp-22-10409-2022-supplement

Atmospheric Chemistry and Physics
Open Access

Supplement of

Sources and processes of water-soluble and water-insoluble organic aerosol in cold season in Beijing, China

Zhiqiang Zhang et al.

Correspondence to: Yele Sun (sunyele@mail.iap.ac.cn)

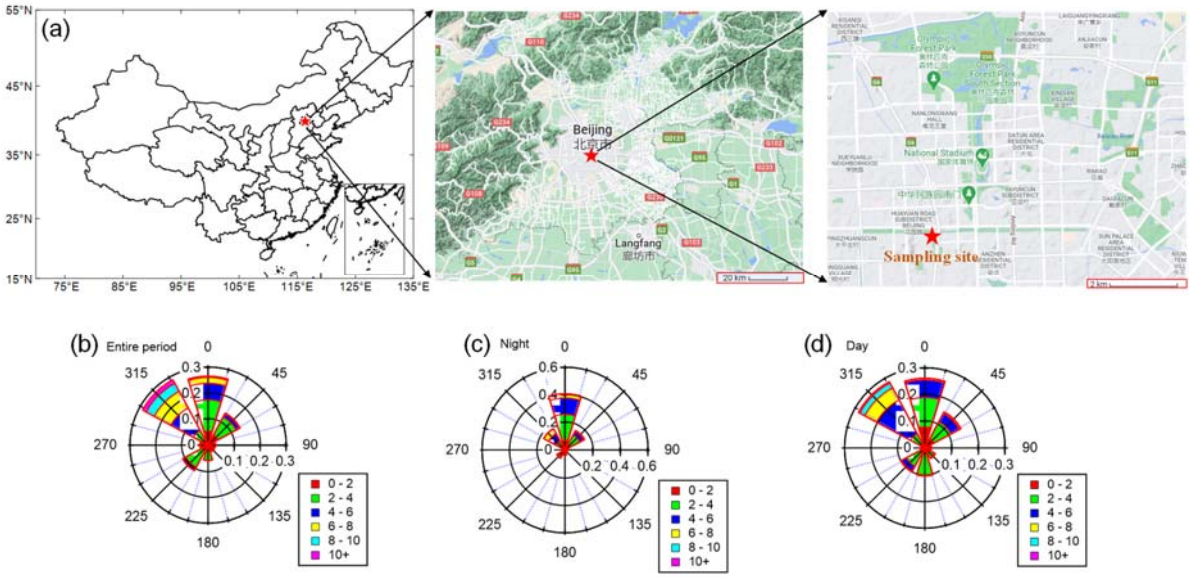

Figure S1. (a) Sampling site position (© Google Maps), and the wind rose plots of (b) the entire period, (c) nighttime (from 6 November to 5 December 2020) and (d) daytime, respectively.

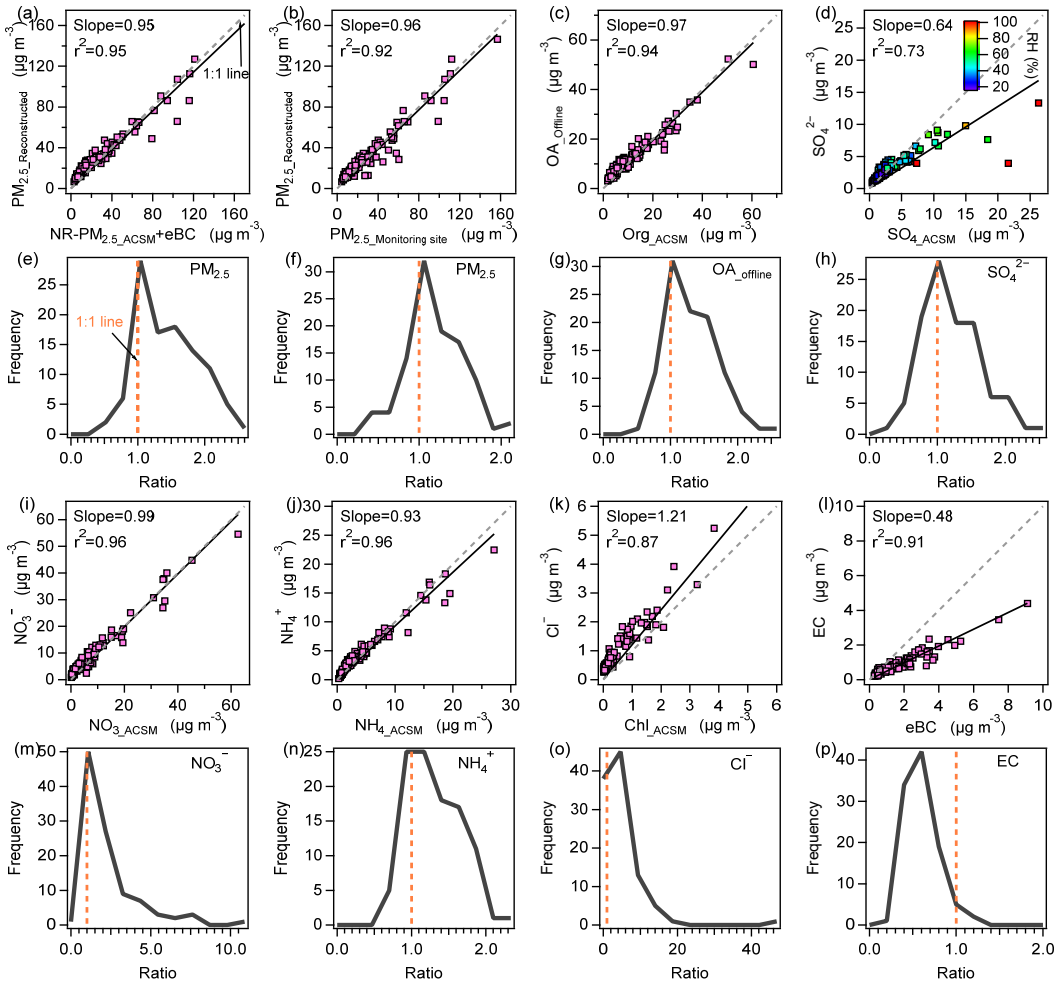

Figure S2. Mass concentration comparisons of online and offline measurements, and the offline-to-online ratio frequency (103 samples in total) distribution.

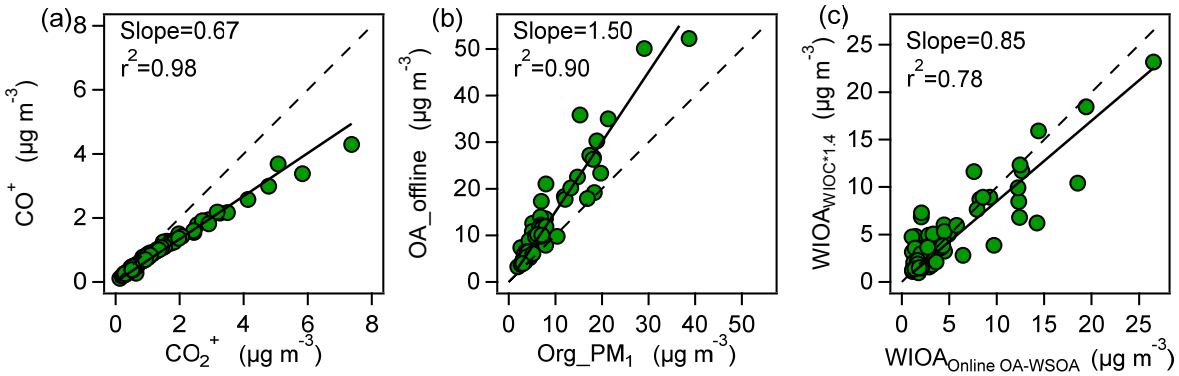

Figure S3. Scatter plots of (a) CO^+ vs. CO_2^+ in WSOA in this study, (b) offline-reconstructed OA (WSOA + WIOA) vs. Org in PM_1 measured with AMS, and (c) reconstructed WIOA (WIOC × 1.4) vs. WIOA calculated from the difference between OA and WSOA. The dashed lines indicate the 1:1 lines.

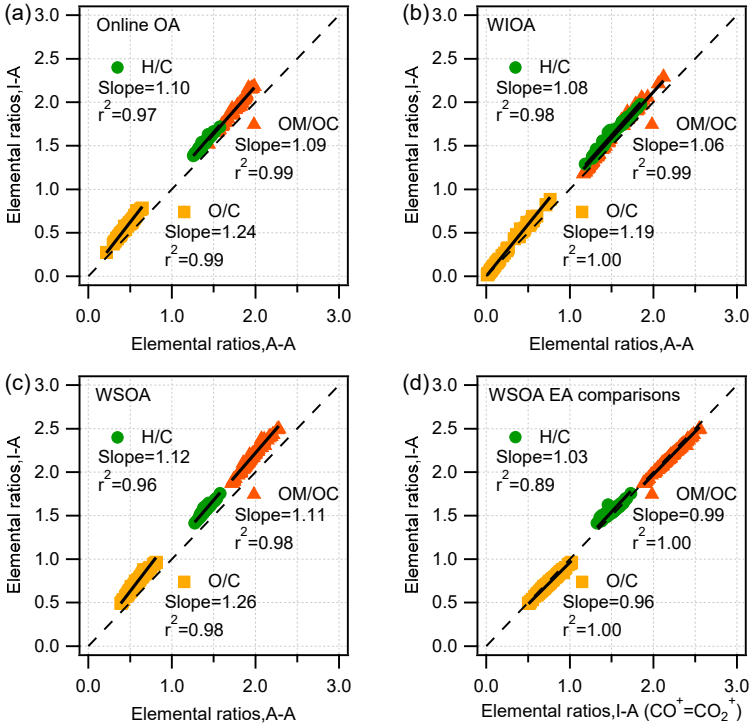

Figure S4. Elemental ratio comparisons of I-A method and A-A method of (a) online OA, (b) WIOA, (c) WSOA (CO^+ use original values). Panel (d) shows the WSOA elemental ratio comparisons when CO^+ use original values and when CO^+ values are equal to CO_2^+ values.

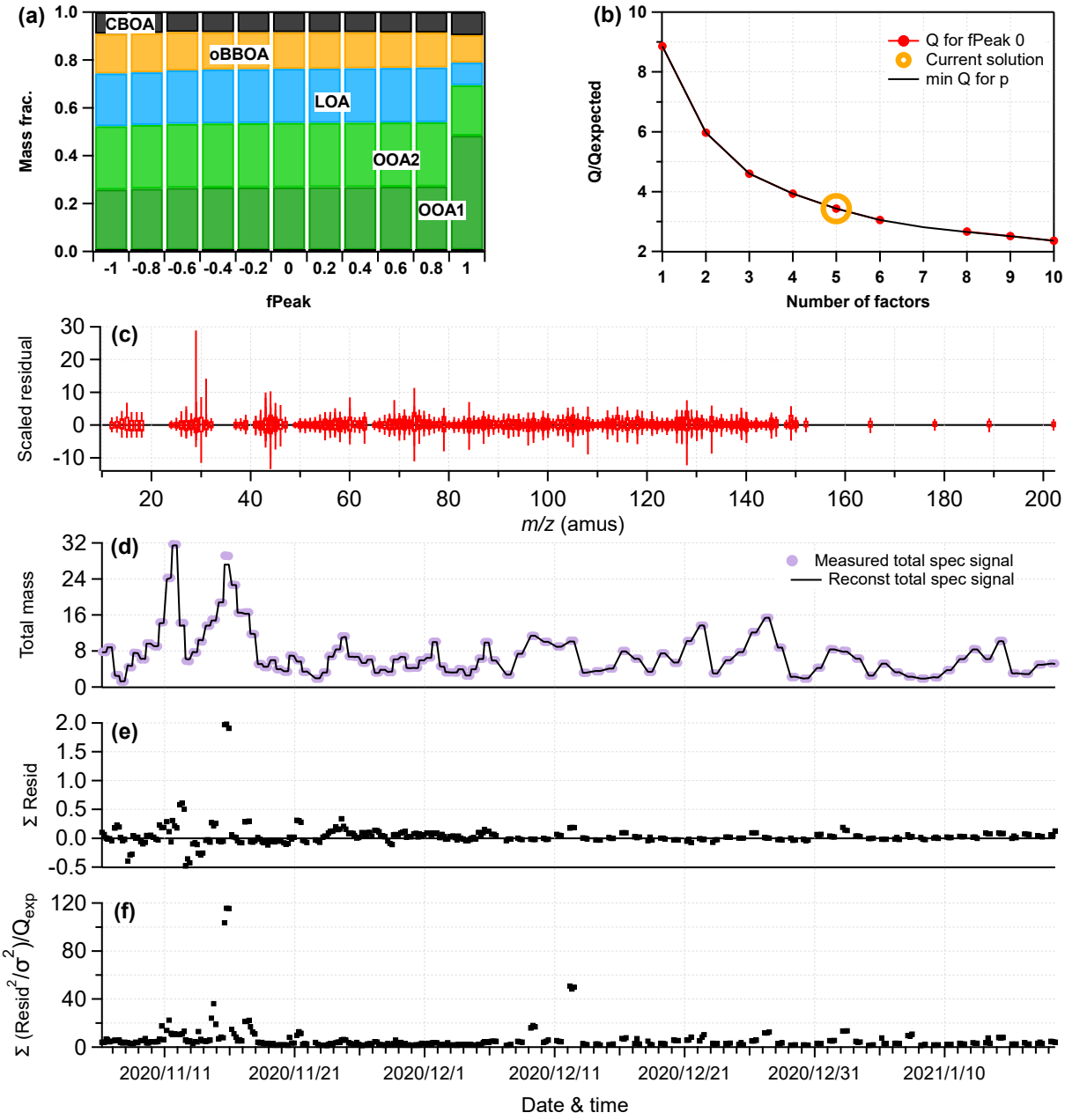

Figure S5. Diagnostic plots of PMF results for 5-factor solution: (a) fractions of OA factors vs. fpeak; (b) Q/Q_{exp} as a function of number of factors selected for PMF modeling; (c) box and whiskers (± 25% of box) presenting the distribution of scaled residuals for each *m/z*; (d) time series of the measured organic mass and reconstructed (reconstructed WSOA = OOA1 + OOA2 + LOA + oBBOA + CBOA) organic mass; (e) time series of the residuals (residuals = measured mass – reconstructed mass); (f) time series of Q/Q_{exp}.

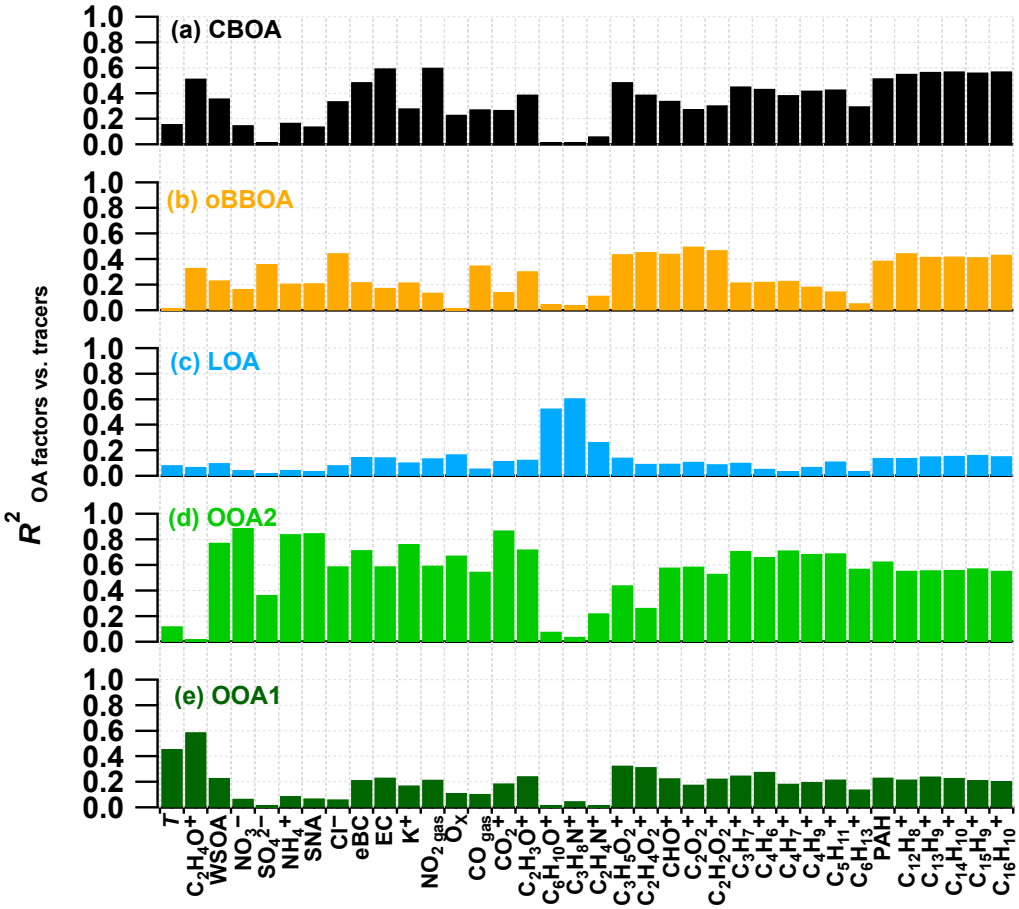

Figure S6. Correlations (R^2) between WSOA factors and common tracers.

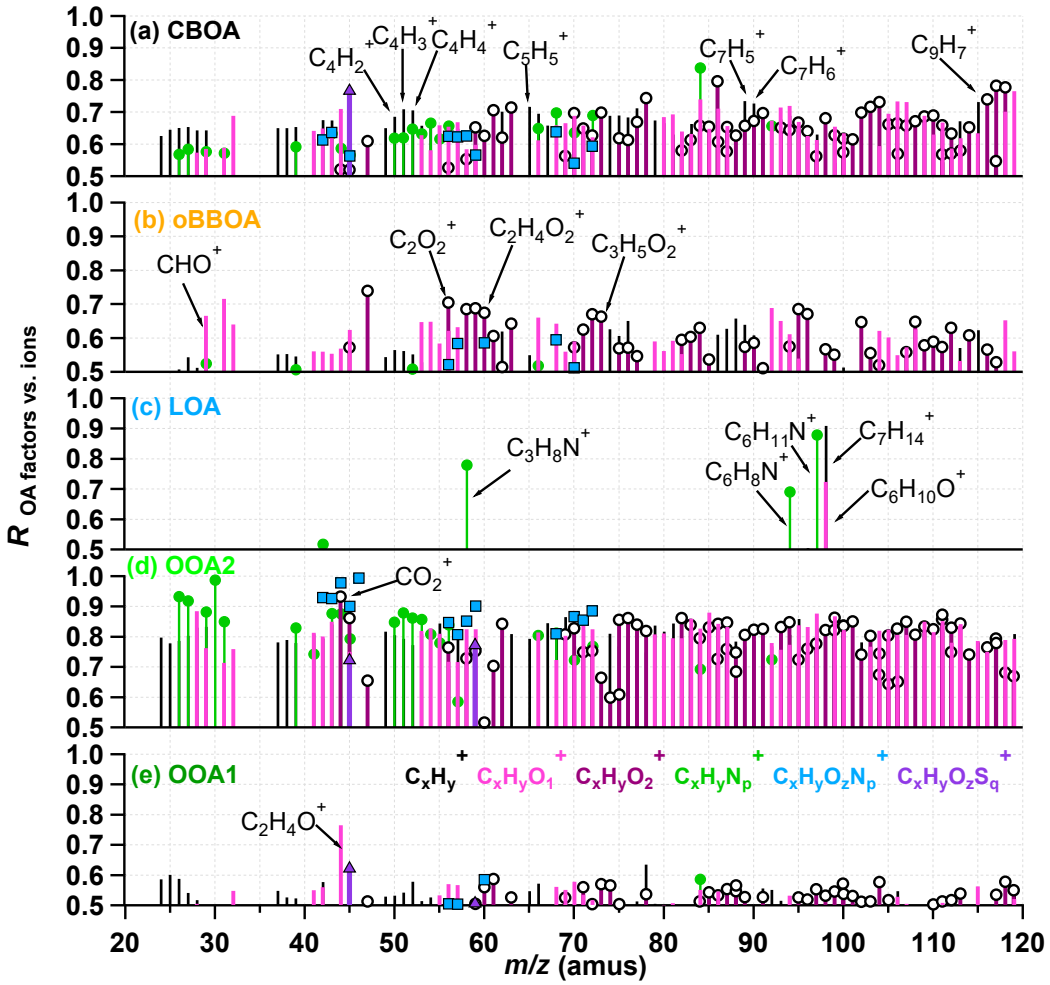

Figure S7. Correlation (R > 0.5) of WSOA factors and individual fragment up to m/z 120.

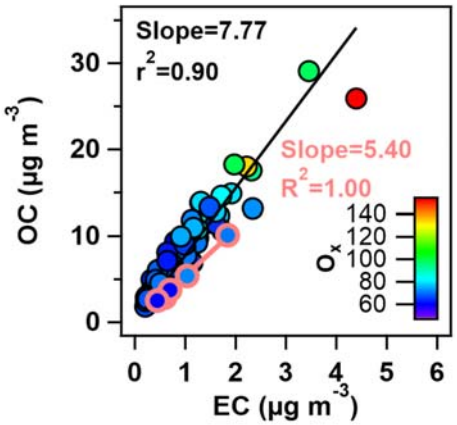

Figure S8. EC-tracer method (OC vs. EC), the points with pink edges have the least OC/EC ratios.

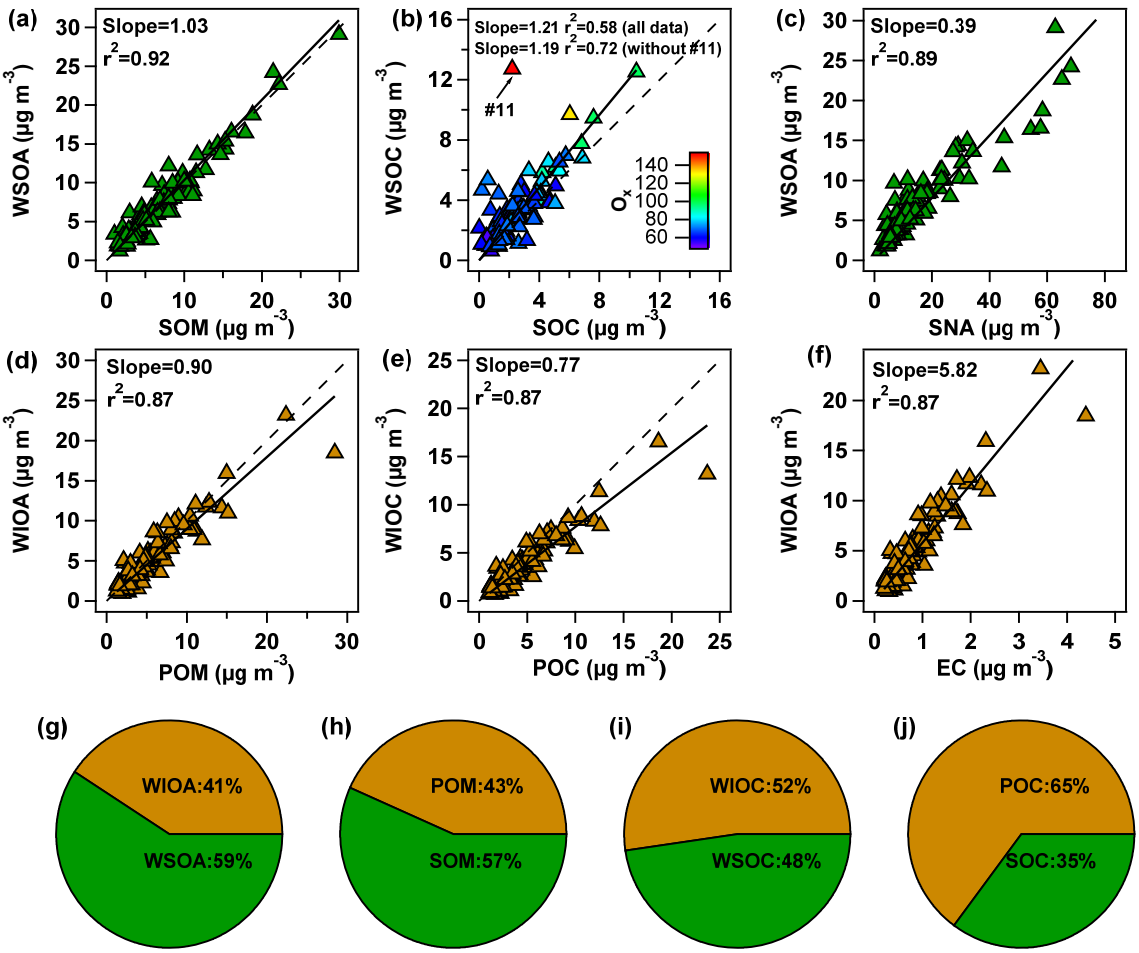

Figure S9. Scatter plots that compare (a) WSOA vs. SOM, (b) WSOC vs. SOC, (c) WSOA vs. SNA, (d) WIOA vs. POM, (e) WIOC vs. POC and (f) WIOA vs. EC, as well as composition pie charts of (g) WIOA & WSOA, (h) POM & SOM, (i) WIOC & WSOC and (j) POC & SOC. The black dashed lines indicate the 1:1 lines.

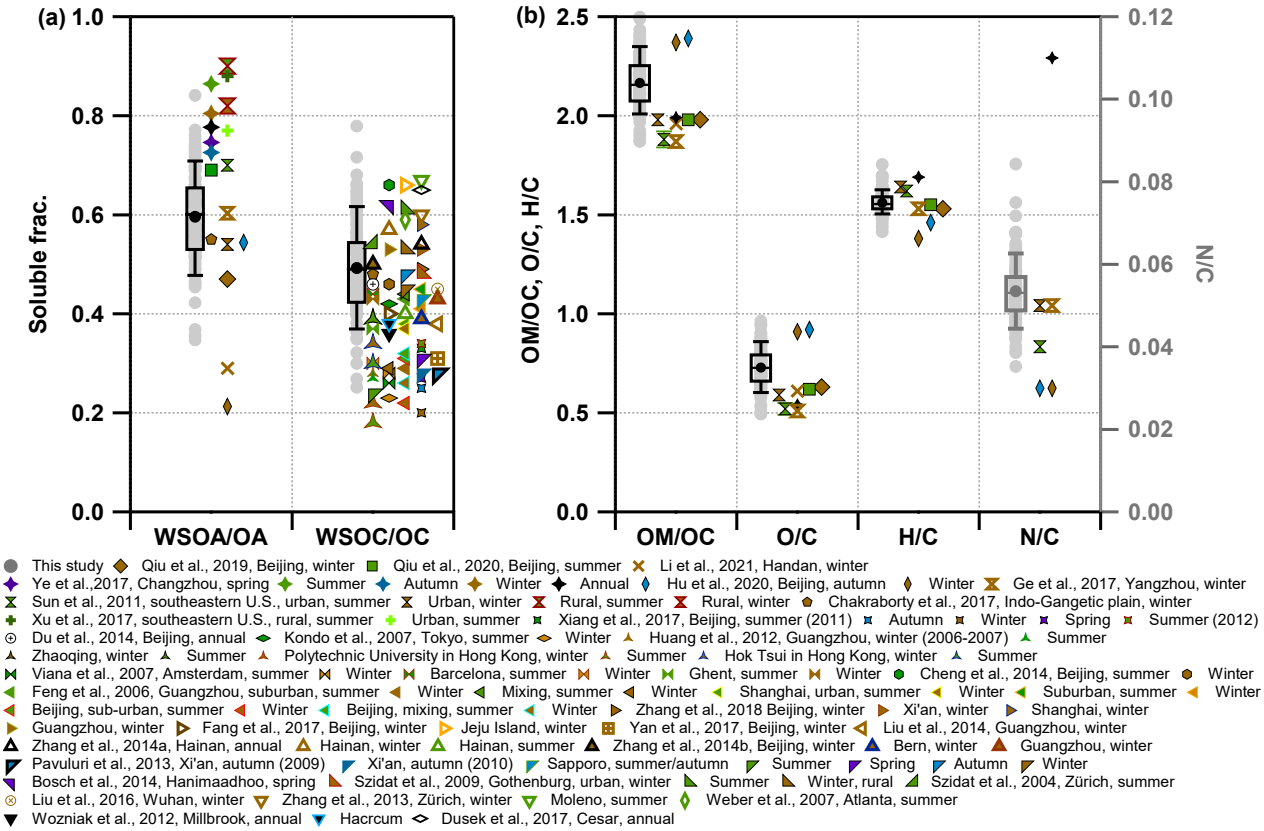

Figure S10. The same picture as Fig. 2, and the detailed references are listed below (Qiu et al., 2019; Qiu et al., 2020; Li et al., 2021; Ye et al., 2017; Hu et al., 2020; Ge et al., 2017; Sun et al., 2011; Chakraborty et al., 2017; Xu et al., 2017; Xiang et al., 2017; Du et al., 2014; Kondo et al., 2007; Huang et al., 2012; Viana et al., 2007; Cheng et al., 2014; Feng et al., 2006; Zhang et al., 2018; Fang et al., 2017; Yan et al., 2017; Liu et al., 2014; Zhang et al., 2014a; Zhang et al., 2014b; Pavuluri et al., 2013; Bosch et al., 2014; Szidat et al., 2009; Szidat et al., 2004; Liu et al., 2016; Zhang et al., 2013; Weber et al., 2007; Wozniak et al., 2012; Dusek et al., 2017).

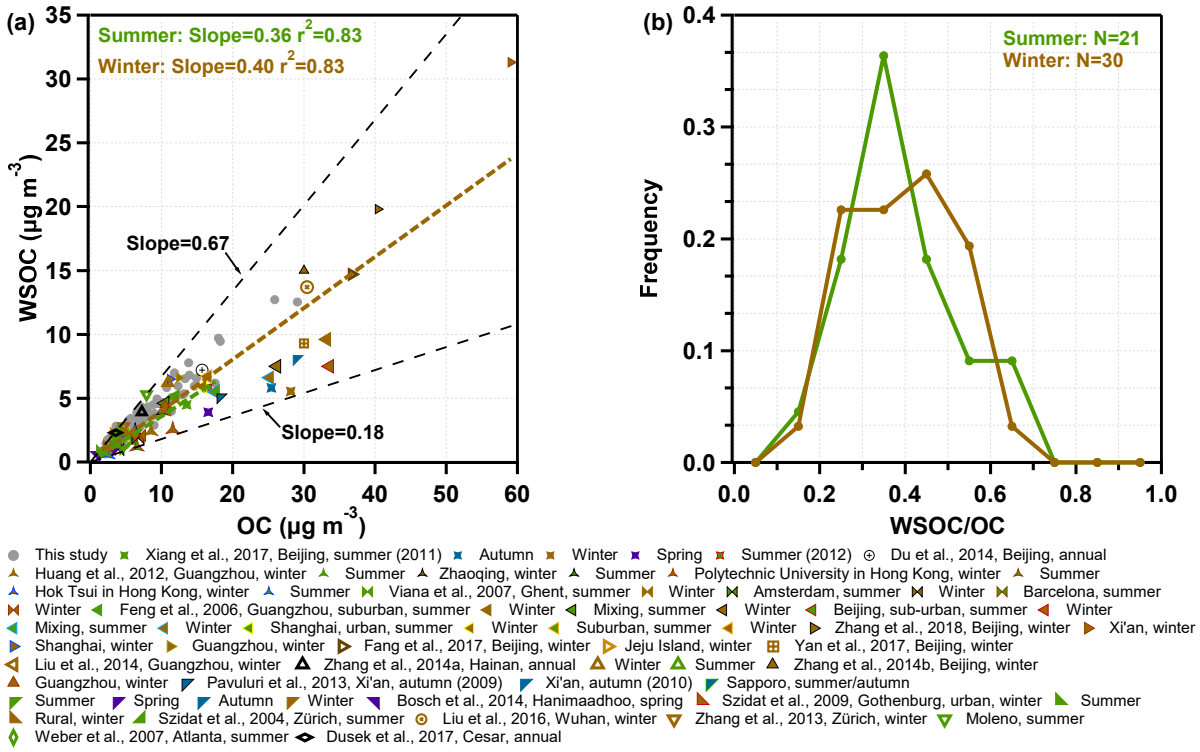

Figure S11. WSOC and OC values summarized from the previous studies (Xiang et al., 2017; Du et al., 2014; Huang et al., 2012; Viana et al., 2007; Feng et al., 2006; Zhang et al., 2018; Fang et al., 2017; Yan et al., 2017; Liu et al., 2014; Zhang et al., 2014a; Zhang et al., 2014b; Pavuluri et al., 2013; Bosch et al., 2014; Szidat et al., 2009; Szidat et al., 2004; Liu et al., 2016; Zhang et al., 2013; Weber et al., 2007; Dusek et al., 2017), the multiple datasets in summer and winter are fitted for comparison in panel (a), and the frequency distribution of WSOC/OC in summer and winter are shown in panel (b). Colored markers represent data from previous studies, which are colored in purple in spring, green in summer, blue in autumn and brown in winter, the data across the year are in black. The results of different seasons and different sites in the same reference are shown with different edge colors in panel (a).

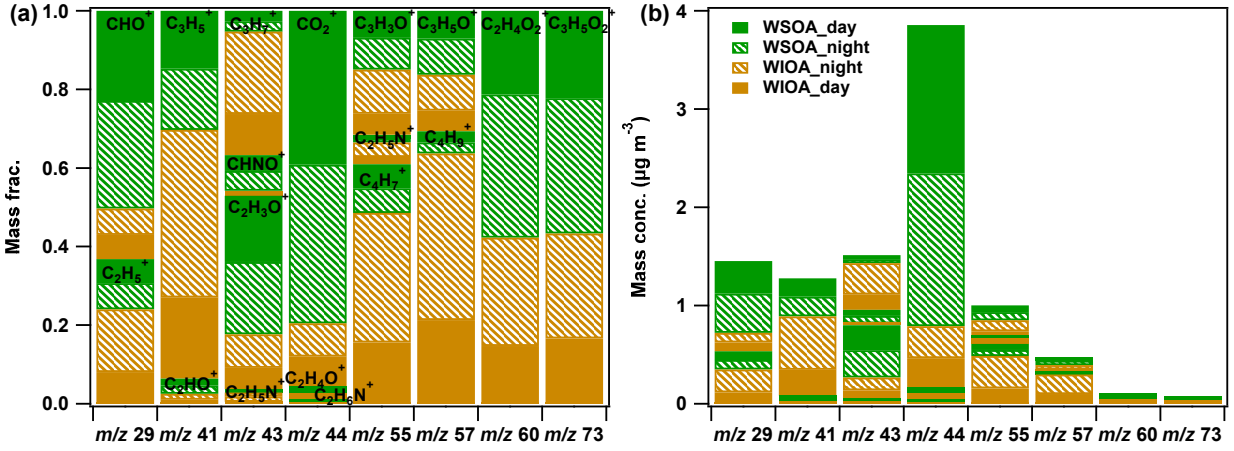

Figure S12. (a) Mass fractions (WSOA_day + WSOA_night + WIOA_night + WIOA_day) and (b) concentrations in *m/z* 29, *m/z* 41, *m/z* 43, *m/z* 44, *m/z* 55, *m/z* 57, *m/z* 60 and *m/z* 73.

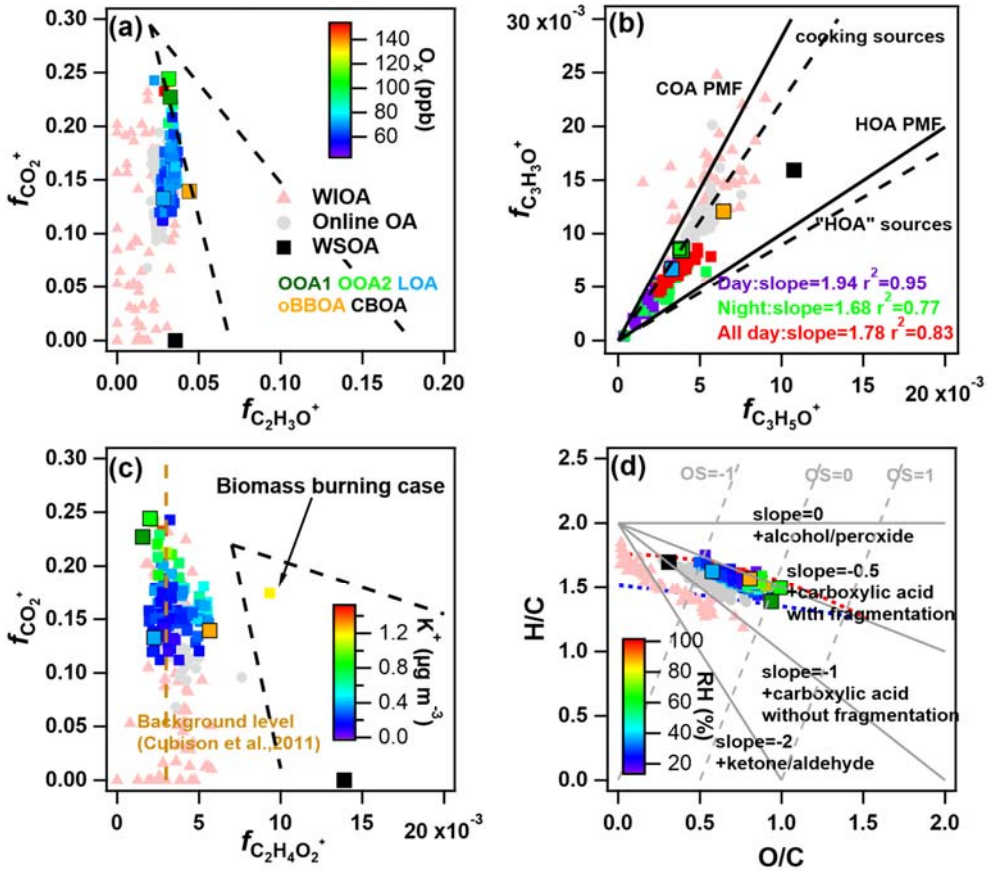

Figure S13. Triangle plots of main fragments corresponding to the unit *m/z*s in Fig. 7, including (a) f_{CO2}^+ vs. f_{C2H3O}^+, (b) f_{C3H3O}^+ vs. f_{C3H5O}^+, (c) f_{CO2}^+ vs. f_{C2H4O2}^+. Panel (d) shows the Van Krevelen diagram, in which the WSOA data are colored by RH. The reference lines are the same as the lines in Fig. 7.

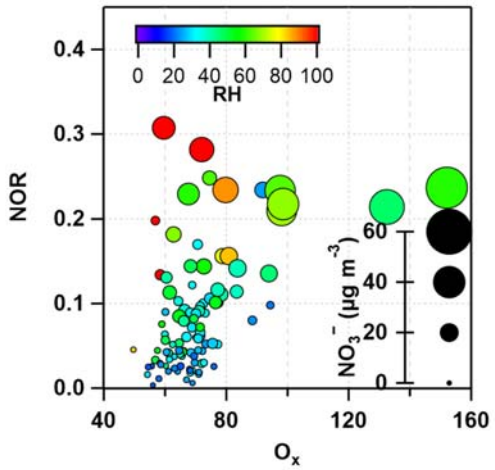

Figure S14. The nitrogen oxidation ratio (NOR) variation as a function of O_x, the data are colored by RH, and the size of markers indicates the mass concentration of NO_3^-.

Table S1. Night-day differences of average values of offline-measured species, elemental ratios (from 6 November 2020 to 5 December 2020, I-A method, CO^+ use original values) and online-measured meteorological parameters and gases, and the average values of the entire time and each divided episode, values of one standard deviation are also shown in the table.

Species	Night	Day	Night-day absolute change	Night-day relative change	Entire period	P1	P2	P3	P4
$PM_{2.5}$ and components (μg m^{-3})									
$PM_{2.5}$	37.2 ± 33.3	34.6 ± 28.7	2.6	7.5%	32.6 ± 26.0	73.1 ± 37.7	126.9	21.9 ± 9.0	28.4 ± 16.6
OA_offline	15.2 ± 12.2	12.2 ± 8.8	3.0	24.7%	12.6 ± 9.0	26.2 ± 12.4	52.3	8.2 ± 3.8	11.3 ± 6.0
WSOA	8.8 ± 7.0	8.0 ± 5.9	0.8	9.8%	7.5 ± 5.5	16.3 ± 7.4	29.1	5.2 ± 2.1	6.3 ± 3.4
WIOA	6.4 ± 5.4	4.2 ± 3.0	2.2	53.3%	5.1 ± 3.8	10.0 ± 5.5	23.2	3.0 ± 1.9	5.0 ± 2.8
SO_4^{2-}	3.4 ± 2.0	3.7 ± 2.4	–0.4	–9.4%	3.5 ± 2.1	5.5 ± 3.1	8.4	3.1 ± 0.8	3.4 ± 2.0
NO_3^-	10.0 ± 12.4	10.6 ± 11.9	–0.6	–5.6%	8.9 ± 9.9	24.5 ± 15.7	37.5	5.4 ± 2.9	7.1 ± 5.3
NH_4^+	4.9 ± 5.2	4.9 ± 4.9	0.02	0.4%	4.3 ± 4.2	10.9 ± 6.3	16.9	2.8 ± 1.4	3.6 ± 2.6
Cl^-	1.2 ± 1.2	0.9 ± 0.7	0.3	28.5%	1.1 ± 0.9	2.0 ± 1.4	5.2	0.7 ± 0.3	1.1 ± 0.8
EC	1.1 ± 1.0	0.8 ± 0.5	0.3	44.3%	0.8 ± 0.7	1.7 ± 1.0	3.5	0.6 ± 0.3	0.7 ± 0.5
Other ions	1.4 ± 0.8	1.5 ± 0.7	–0.1	–5.7%	1.3 ± 0.5	2.2 ± 0.7	3.2	1.1 ± 0.3	1.2 ± 0.4
WSOA factors (μg m^{-3})									
OOA1	2.7 ± 2.4	2.5 ± 2.2	0.2	6.8%	2.0 ± 1.9	4.6 ± 2.5	10.0	1.2 ± 0.9	1.2 ± 0.7
OOA2	2.5 ± 5.7	2.4 ± 5.1	0.1	4.3%	2.0 ± 4.3	8.2 ± 8.0	7.5	0.3 ± 0.5	1.4 ± 2.0
LOA	1.8 ± 1.1	2.2 ± 1.4	–0.4	–17.7%	1.7 ± 1.0	0.9 ± 1.0	0.9	2.9 ± 0.6	1.3 ± 0.3
oBBOA	0.9 ± 1.4	0.4 ± 0.6	0.5	110.0%	1.1 ± 1.3	1.3 ± 1.7	7.0	0.4 ± 0.5	1.8 ± 1.2
CBOA	0.8 ± 0.8	0.5 ± 0.5	0.4	85.3%	0.6 ± 0.6	1.2 ± 0.7	1.8	0.3 ± 0.4	0.6 ± 0.6
Other ions (μg m^{-3})									
Ca^{2+}	0.17 ± 0.14	0.17 ± 0.14	–0.003	–1.7%	0.22 ± 0.16	0.23 ± 0.12	0.22	0.10 ± 0.05	0.29 ± 0.16
F^-	0.15 ± 0.06	0.17 ± 0.04	–0.02	–10.8%	0.14 ± 0.05	0.22 ± 0.07	0.35	0.15 ± 0.02	0.11 ± 0.02
Na^+	0.13 ± 0.12	0.10 ± 0.09	0.03	28.8%	0.15 ± 0.12	0.24 ± 0.14	0.57	0.07 ± 0.04	0.19 ± 0.11
NO_2^-	0.07 ± 0.07	0.12 ± 0.09	–0.05	–39.6%	0.08 ± 0.07	0.11 ± 0.09	0	0.08 ± 0.08	0.07 ± 0.04
K^+	0.42 ± 0.32	0.35 ± 0.26	0.07	18.7%	0.35 ± 0.24	0.74 ± 0.34	1.19	0.24 ± 0.08	0.30 ± 0.14
Mg^{2+}	0.45 ± 0.17	0.56 ± 0.12	–0.11	–19.6%	0.40 ± 0.17	0.62 ± 0.13	0.85	0.46 ± 0.16	0.27 ± 0.03
Elemental ratios									
OM/OC	2.15 ± 0.14	2.16 ± 0.17	–0.01	–0.7%	2.16 ± 0.13	2.34 ± 0.11	2.32	2.07 ± 0.09	2.18 ± 0.10
O/C	0.72 ± 0.10	0.73 ± 0.13	–0.01	–1.5%	0.73 ± 0.10	0.86 ± 0.07	0.85	0.65 ± 0.07	0.74 ± 0.07
H/C	1.56 ± 0.06	1.56 ± 0.07	–0.002	–0.1%	1.56 ± 0.05	1.51 ± 0.04	1.55	1.59 ± 0.05	1.56 ± 0.03
N/C	0.055 ± 0.008	0.055 ± 0.009	–0.000	–0.1%	0.053 ± 0.008	0.059 ± 0.013	0.053	0.055 ± 0.003	0.052 ± 0.006
Meteorological parameters									
RH (%)	48.6 ± 20.2	43.1 ± 23.9	5.4	12.5%	40.5 ± 19.7	61.3 ± 25.3	69.9	43.9 ± 18.0	33.5 ± 12.9
T (°C)	5.0 ± 5.0	7.0 ± 5.4	–2.0	–29.0%	2.6 ± 6.2	11.1 ± 2.1	10.1	2.2 ± 2.6	–1.8 ± 4.0
WS (m s^{-1})	3.5 ± 1.3	3.7 ± 1.5	–0.11	–3.0%	3.9 ± 1.6	2.7 ± 0.9	2.2	3.9 ± 1.3	4.3 ± 1.7
Gases (ppb)									
NO_2	53.5 ± 28.8	38.4 ± 27.7	15.1	39.4%	42.6 ± 25.5	78.0 ± 29.5	96.6	31.2 ± 16.1	38.5 ± 19.2
CO	63.5 ± 43.4	56.6 ± 41.2	6.9	12.2%	58.9 ± 37.9	110.0 ± 50.0	181.4	41.1 ± 14.9	57.0 ± 31.5
O_3	17.1 ± 15.8	35.0 ± 17.4	–17.9	–51.1%	28.0 ± 17.5	11.1 ± 14.2	1.5	32.6 ± 16.7	30.2 ± 15.8
SO_2	3.7 ± 1.9	3.8 ± 2.3	–0.1	–2.6%	4.6 ± 2.5	4.5 ± 2.3	3.4	3.6 ± 2.1	5.8 ± 2.6
O_x	70.6 ± 19.0	73.4 ± 16.2	–2.8	–3.8%	70.6 ± 14.1	89.1 ± 24.0	98.1	63.9 ± 6.0	68.7 ± 6.6

References

Bosch, C., Andersson, A., Kirillova, E. N., Budhavant, K., Tiwari, S., Praveen, P. S., Russell, L. M., Beres, N. D., Ramanathan, V., and Gustafsson, Ö.: Source-diagnostic dual-isotope composition and optical properties of water-soluble organic carbon and elemental carbon in the South Asian outflow intercepted over the Indian Ocean, J. Geophys. Res.: Atmos., 119, 11,743-711,759, https://doi.org/10.1002/2014JD022127, 2014.

Chakraborty, A., Rajeev, P., Rajput, P., and Gupta, T.: Water soluble organic aerosols in Indo Gangetic Plain (IGP): insights from aerosol mass spectrometry, Sci. Total Environ., 599-600, 1573-1582, https://doi.org/10.1016/j.scitotenv.2017.05.142, 2017.

Cheng, Y., Engling, G., He, K.-b., Duan, F.-k., Du, Z.-y., Ma, Y.-l., Liang, L.-l., Lu, Z.-f., Liu, J.-m., Zheng, M., and Weber, R. J.: The characteristics of Beijing aerosol during two distinct episodes: impacts of biomass burning and fireworks, Environ. Pollut., 185, 149-157, https://doi.org/10.1016/j.envpol.2013.10.037, 2014.

Du, Z., He, K., Cheng, Y., Duan, F., Ma, Y., Liu, J., Zhang, X., Zheng, M., and Weber, R.: A yearlong study of water-soluble organic carbon in Beijing I: sources and its primary vs. secondary nature, Atmos. Environ., 92, 514-521, https://doi.org/10.1016/j.atmosenv.2014.04.060, 2014.

Dusek, U., Hitzenberger, R., Kasper-Giebl, A., Kistler, M., Meijer, H. A. J., Szidat, S., Wacker, L., Holzinger, R., and Röckmann, T.: Sources and formation mechanisms of carbonaceous aerosol at a regional background site in the Netherlands: insights from a year-long radiocarbon study, Atmos. Chem. Phys., 17, 3233-3251, https://doi.org/10.5194/acp-17-3233-2017, 2017.

Fang, W., Andersson, A., Zheng, M., Lee, M., Holmstrand, H., Kim, S.-W., Du, K., and Gustafsson, Ö.: Divergent evolution of carbonaceous aerosols during dispersal of East Asian haze, Sci. Rep., 7, 10422, https://doi.org/10.1038/s41598-017-10766-4, 2017.

Feng, J., Hu, M., Chan, C. K., Lau, P. S., Fang, M., He, L., and Tang, X.: A comparative study of the organic matter in $PM_{2.5}$ from three Chinese megacities in three different climatic zones, Atmos. Environ., 40, 3983-3994, https://doi.org/10.1016/j.atmosenv.2006.02.017, 2006.

Ge, X., Li, L., Chen, Y., Chen, H., Wu, D., Wang, J., Xie, X., Ge, S., Ye, Z., Xu, J., and Chen, M.: Aerosol characteristics and sources in Yangzhou, China resolved by offline aerosol mass spectrometry and other techniques, Environ. Pollut., 225, 74-85, https://doi.org/10.1016/j.envpol.2017.03.044, 2017.

Hu, R., Xu, Q., Wang, S., Hua, Y., Bhattarai, N., Jiang, J., Song, Y., Daellenbach, K. R., Qi, L., Prevot, A. S. H., and Hao, J.: Chemical characteristics and sources of water-soluble organic aerosol in southwest suburb of Beijing, J. Environ. Sci., 95, 99-110, https://doi.org/10.1016/j.jes.2020.04.004, 2020.

Huang, H., Ho, K. F., Lee, S. C., Tsang, P. K., Ho, S. S. H., Zou, C. W., Zou, S. C., Cao, J. J., and Xu, H. M.: Characteristics of carbonaceous aerosol in $PM_{2.5}$: Pearl Delta River region, China, Atmos. Res., 104-105, 227-236, https://doi.org/10.1016/j.atmosres.2011.10.016, 2012.

Kondo, Y., Miyazaki, Y., Takegawa, N., Miyakawa, T., Weber, R. J., Jimenez, J. L., Zhang, Q., and Worsnop, D. R.: Oxygenated and water-soluble organic aerosols in Tokyo, J. Geophys. Res.: Atmos., 112, https://doi.org/10.1029/2006JD007056, 2007.

Li, H., Zhang, Q., Jiang, W., Collier, S., Sun, Y., Zhang, Q., and He, K.: Characteristics and sources of

water-soluble organic aerosol in a heavily polluted environment in Northern China, Sci. Total Environ., 758, 143970, https://doi.org/10.1016/j.scitotenv.2020.143970, 2021.

Liu, J., Li, J., Zhang, Y., Liu, D., Ding, P., Shen, C., Shen, K., He, Q., Ding, X., Wang, X., Chen, D., Szidat, S., and Zhang, G.: Source apportionment using radiocarbon and organic tracers for $PM_{2.5}$ carbonaceous aerosols in guangzhou, South China: contrasting local- and regional-scale haze events, Environ. Sci. Technol., 48, 12002-12011, https://doi.org/10.1021/es503102w, 2014.

Liu, J., Li, J., Vonwiller, M., Liu, D., Cheng, H., Shen, K., Salazar, G., Agrios, K., Zhang, Y., He, Q., Ding, X., Zhong, G., Wang, X., Szidat, S., and Zhang, G.: The importance of non-fossil sources in carbonaceous aerosols in a megacity of central China during the 2013 winter haze episode: a source apportionment constrained by radiocarbon and organic tracers, Atmos. Environ., 144, 60-68, https://doi.org/10.1016/j.atmosenv.2016.08.068, 2016.

Pavuluri, C. M., Kawamura, K., Uchida, M., Kondo, M., and Fu, P.: Enhanced modern carbon and biogenic organic tracers in Northeast Asian aerosols during spring/summer, J. Geophys. Res.: Atmos., 118, 2362-2371, https://doi.org/10.1002/jgrd.50244, 2013.

Qiu, Y., Xu, W., Jia, L., He, Y., Fu, P., Zhang, Q., Xie, Q., Hou, S., Xie, C., Xu, Y., Wang, Z., Worsnop, D. R., and Sun, Y.: Molecular composition and sources of water-soluble organic aerosol in summer in Beijing, Chemosphere, 255, 126850, https://doi.org/10.1016/j.chemosphere.2020.126850, 2020.

Qiu, Y., Xie, Q., Wang, J., Xu, W., Li, L., Wang, Q., Zhao, J., Chen, Y., Chen, Y., Wu, Y., Du, W., Zhou, W., Lee, J., Zhao, C., Ge, X., Fu, P., Wang, Z., Worsnop, D. R., and Sun, Y.: Vertical characterization and source apportionment of water-soluble organic aerosol with high-resolution aerosol mass spectrometry in Beijing, China, ACS Earth Space Chem., 3, 273-284, https://doi.org/10.1021/acsearthspacechem.8b00155, 2019.

Sun, Y., Zhang, Q., Zheng, M., Ding, X., Edgerton, E. S., and Wang, X.: Characterization and source apportionment of water-soluble organic matter in atmospheric fine particles ($PM_{2.5}$) with high-resolution aerosol mass spectrometry and GC–MS, Environ. Sci. Technol., 45, 4854-4861, https://doi.org/10.1021/es200162h, 2011.

Szidat, S., Ruff, M., Perron, N., Wacker, L., Synal, H. A., Hallquist, M., Shannigrahi, A. S., Yttri, K. E., Dye, C., and Simpson, D.: Fossil and non-fossil sources of organic carbon (OC) and elemental carbon (EC) in Göteborg, Sweden, Atmos. Chem. Phys., 9, 1521-1535, https://doi.org/10.5194/acp-9-1521-2009, 2009.

Szidat, S., Jenk, T. M., Gäggeler, H. W., Synal, H. A., Fisseha, R., Baltensperger, U., Kalberer, M., Samburova, V., Wacker, L., Saurer, M., Schwikowski, M., and Hajdas, I.: Source apportionment of aerosols by ^{14}C measurements in different carbonaceous particle fractions, Radiocarbon, 46, 475-484, https://doi.org/10.1017/S0033822200039783, 2004.

Viana, M., Maenhaut, W., ten Brink, H. M., Chi, X., Weijers, E., Querol, X., Alastuey, A., Mikuška, P., and Večeřa, Z.: Comparative analysis of organic and elemental carbon concentrations in carbonaceous aerosols in three European cities, Atmos. Environ., 41, 5972-5983, https://doi.org/10.1016/j.atmosenv.2007.03.035, 2007.

Weber, R. J., Sullivan, A. P., Peltier, R. E., Russell, A., Yan, B., Zheng, M., de Gouw, J., Warneke, C., Brock, C., Holloway, J. S., Atlas, E. L., and Edgerton, E.: A study of secondary organic aerosol formation in the anthropogenic-influenced southeastern United States, J. Geophys. Res.: Atmos., 112, https://doi.org/10.1029/2007JD008408, 2007.

Wozniak, A. S., Bauer, J. E., and Dickhut, R. M.: Characteristics of water-soluble organic carbon associated with aerosol particles in the eastern United States, Atmos. Environ., 46, 181-188,

https://doi.org/10.1016/j.atmosenv.2011.10.001, 2012.

Xiang, P., Zhou, X., Duan, J., Tan, J., He, K., Yuan, C., Ma, Y., and Zhang, Y.: Chemical characteristics of water-soluble organic compounds (WSOC) in $PM_{2.5}$ in Beijing, China: 2011–2012, Atmos. Res., 183, 104-112, https://doi.org/10.1016/j.atmosres.2016.08.020, 2017.

Xu, L., Guo, H., Weber, R. J., and Ng, N. L.: Chemical characterization of water-soluble organic aerosol in contrasting rural and urban environments in the southeastern United States, Environ. Sci. Technol., 51, 78-88, https://doi.org/10.1021/acs.est.6b05002, 2017.

Yan, C., Zheng, M., Bosch, C., Andersson, A., Desyaterik, Y., Sullivan, A. P., Collett, J. L., Zhao, B., Wang, S., He, K., and Gustafsson, Ö.: Important fossil source contribution to brown carbon in Beijing during winter, Sci. Rep., 7, 43182, https://doi.org/10.1038/srep43182, 2017.

Ye, Z., Liu, J., Gu, A., Feng, F., Liu, Y., Bi, C., Xu, J., Li, L., Chen, H., Chen, Y., Dai, L., Zhou, Q., and Ge, X.: Chemical characterization of fine particulate matter in Changzhou, China, and source apportionment with offline aerosol mass spectrometry, Atmos. Chem. Phys., 17, 2573-2592, https://doi.org/10.5194/acp-17-2573-2017, 2017.

Zhang, Y.-L., Li, J., Zhang, G., Zotter, P., Huang, R.-J., Tang, J.-H., Wacker, L., Prévôt, A. S. H., and Szidat, S.: Radiocarbon-based source apportionment of carbonaceous aerosols at a regional background site on Hainan Island, South China, Environ. Sci. Technol., 48, 2651-2659, https://doi.org/10.1021/es4050852, 2014a.

Zhang, Y.-L., Liu, J.-W., Salazar, G. A., Li, J., Zotter, P., Zhang, G., Shen, R.-r., Schäfer, K., Schnelle-Kreis, J., Prévôt, A. S. H., and Szidat, S.: Micro-scale (μg) radiocarbon analysis of water-soluble organic carbon in aerosol samples, Atmos. Environ., 97, 1-5, https://doi.org/10.1016/j.atmosenv.2014.07.059, 2014b.

Zhang, Y. L., Zotter, P., Perron, N., Prévôt, A. S. H., Wacker, L., and Szidat, S.: Fossil and non-fossil sources of different carbonaceous fractions in fine and coarse particles by radiocarbon measurement, Radiocarbon, 55, 1510-1520, https://doi.org/10.1017/S0033822200048438, 2013.

Zhang, Y. L., El-Haddad, I., Huang, R. J., Ho, K. F., Cao, J. J., Han, Y., Zotter, P., Bozzetti, C., Daellenbach, K. R., Slowik, J. G., Salazar, G., Prévôt, A. S. H., and Szidat, S.: Large contribution of fossil fuel derived secondary organic carbon to water soluble organic aerosols in winter haze in China, Atmos. Chem. Phys., 18, 4005-4017, https://doi.org/10.5194/acp-18-4005-2018, 2018.